IIETA International Information and Engineering Technology Association
Advancing the World of Information and Engineering

Journal of New Materials for Electrochemical Systems
Vol. 28, No. 2, April 2025, pp. 211-216
Journal homepage: http://iieta.org/journals/jnmes

The effect substitution of lanthanum-aluminate oxide of the catalytic performance of $La_{1-x}Sr_xAlO_{3-\delta}$ (x = 0.1, 0.2, 0.3) for methane oxidation

Abderezak GUEMACHE [1,*], Mahmoud DRIF [2], Ahmed Bouchelaghem[2], Fares KAHOUL [3], Louanes HAMZIOUI [3]

[1] Laboratory of Water, Environment and Renewable Energies , Pole, Road Bordj Bou Arreridj, M'sila 28000 Algeria
[2]Université de M'Sila, Département D'électronique, Pole, Road Bordj Bou Arreridj, M'sila 28000 Algeria
[3]Université de M'Sila, Département Socle Commun ST, Pole, Road Bordj Bou Arreridj, M'sila 28000 Algeria

Corresponding Author Email:abderezak.guemache@univ-msila.dz

https://doi.org/10.18280/jnmes.v28i2.a10

Received: March 26, 2024
Accepted: Accepted 30, 2025

Keywords:
Perovskite, Co-precipitation, *Specific surface (BET), Catalytic activity.*

ABSTRACT

This work shows the catalytic activity of the methane oxidation reaction on catalytic powders such as perovskite - aluminate oxide $La_{1-x}Sr_xAlO_{3-\delta}$, with x = 0, 0.1, 0.2, 0.3. The $La_{1-x}Sr_xAlO_{3-\delta}$ (0<x<0.3) matrix was prepared by the co-precipitation method, the pure phase was characterized by X-ray diffraction (XRD) , thermal and differential gravimetric analysis (TG/DSC), Fourier transform infrared spectroscopy (FTIR), Specific surface area (BET). SEM micrographs showed spherical grains and uniform. The maximum catalytic activity of the different $La_{1-x}Sr_xAlO_{3-\delta}$catalyst (x = 0.1, 0.2, 0.3) for CH_4 combustion reactions was observed on the surrogate samples (x = 0.1, 0.2, 0.3) by the analytical system used in gas chromatography (GC) (IGC 1025 FL INTER SMAT). A higher degree of substitution produces an increase in catalytic oxidation activity.

1. INTRODUCTION

Catalytic activity of perovskite -based materials (ABO_3) has been widely illuminated in the literature for energy and environmental applications and has been widely used as competitive catalysts in various oxidation reactions due to its unique structure, considerable redox properties and wonderful elasticity of the crystalline network available for cation substitution [1].The perovskite ABO_3 type is considered to have a movement of three dimensional frame structure where sharing the top BO6 octahedral build the structure and ions A are placed in 12- cubes sites last lattice [2].This recently years different chemical methods such as the hydroxide, cyanide nitrate solution[3] carbonate[4] acetate oxalate[5]co - precipitation and homogeneous precipitation of urea followed by a thermal decomposition method[6],these methods should normally be at a low temperature of preparation and highly dispersed decomposition of homogeneous perovskite oxides compared to conventional ceramics.

In the perovskite structure a represents the cation of alkaline earth or alkaline metal while B represents the transition metal. In perovskite, A and/or B-site cations may be substituted by other metal elements, resulting in multi-component oxides($A_{1-x}A'_xB_{1-y}B'yO_3$), which could create structural defects or modify oxidation states (in Site B) [7].

The structure was also used as a catalyst for oxidative coupling of methane and the hydrogenation and hydrogenolysis of hydrocarbons .The catalytic properties of $La_{1-x}M_xCO_{3-\delta}$(M= Na, K, Ce, Ca, Sr, Ba, = 0,0.05,0.1,02,0.3) doped, were studied coupling of the methane reaction[8]. Catalytic plays a very important role in many industrial, energy and environmental applications, in the petrochemical industry, total combustion for energy production, selective catalytic NOx reduction,CO_2reduction. Metal oxide catalysts have become increasingly interested in replacing noble metal catalysts.Along with all perovskite catalysts used for catalytic oxidation of methane on matrix perovskites, $LaMnO_3$ and $LaCoO_3$ have attracted much attention for their excellent catalytic activities and good thermal stability[9].The networked properties of oxygen and the conductivity of the perovskite catalysts' oxygenated ions are key factors in determining catalytic activity and should therefore be precisely controlled for the systematic design of effective catalysts[10].

$La_{1-x}Sr_xAlO_{3-\delta}$ (x = 0,0.1,0.2,0.3) powders prepared by the co - precipitation method are used as electrodes to monitor the electrochemical evolution of oxygen in KOH 1M solution at 25°C.The results showed that the effect of the substitution rate x of the electrode increases the electrochemical activity is produced an amount of oxygen at the surface of the interesting electrode [11]. In other cases the electrochemical activity of the $Ca_{1-x}Sr_xMnO_3$ oxides synthesized by the co-precipitation method is preferable for the most strontium-rich for better oxygen evolution[12] in 0.1 M KOH at 25°C.It also has potential application to the Fuell cell solid oxide (SOFC) and also as an electrolyte material when it is doped with the cation such as $Sr^{2+}$and Mg^{2+} due to the improvement of the conductivity of the oxygen at temperatures (600-800°C)[13]. The oxygen reduction reaction is one of the most important electrochemical reactions in energy conversion and storage technologies, such as fuel cells and metal–air batteries [14].

The work we have carried out applies to lanthanum, strontium and aluminum oxides. It consists of determining the optimal conditions for the synthesis of these materials and studying their catalytic behavior with a view to possible

applications as a catalyst to increase catalytic performance for the oxidation of methane.

2. EXPERIMENTAL

2.1 Chemicals

Obtaining the amorphous precursor Nitro - hydroxyde already used to produce $LaAlO_3$,$SrMnO_3$[15]. We used La $(NO_3)_2$ $6H_2O$,purity >99% supplied by Prolabo and Al $(NO_3)_2$ 9 H_2O purity >99% supplied by Prolabo and Sr $(NO_3)_2$ purity > 99% supplied by Sigma-Aldrich and NaOH purity >98% supplied by Sigma-Aldrich

2.2 Preparation

$La_{1-x}Sr_xAlO_{3-\delta}$ (x = 0,0.1,0.2,0.3) were synthesized using aqueous co-precipitation method The precipitate was prepared using stoichiometric amounts of analytical grade $La(NO_3)_2$,$6H_2O$,$Al(NO_3)_3$,$9H_2O$ and $Sr(NO_3)_2$,by dropping slowly at a rate 0.5cm^3/min into dilute KOH solution 14N.The pH value was kept in a range of 10-12 by adjusting the amount of KOH to from white precipitates. After the reaction was completed, the white precipitates were then washed in distilled water by centrifugation for 15min/6000r/min. Subsequently, the precipitates were dried at 110°C for 24 h and then fired at 1000°C for 6h.

2.3 Characterisation

Thermo gravimetric analysis (TGA) and differential scanning calorimetry (DSC) were carried out for the hydroxide precursor at heating rate of 10°C/min under static helium on NETZSCH STA 409C/CD.The Infrared spectra a SHIMADZU, FTIR - 8000, Spectrometer (400-4000 cm^{-1}) Samples were prepared as KBr pellets. The formation of perovskite phase was confirmed by recording the XRD powder pattern of the base oxide on an X-ray diffractometer (BRUERK AXS D8Advance) using Cu-Kα radiation (λ=1.5406Å). The specifique surface area of the powder was measured by the BET technique with nitrogen QUANTACHROME AUTOSORB I. The catalytic properties of the lanthanum- and aluminate-based mixed oxides doped by strontium with respect to the methane oxidation reaction were determined by gas chromatography (GC). Scanning electron microscopy (MEB) JEOL JSM 7001F was used to study the morphology of the by aqueous co-precipitation method.For catalytic activity investigations, the oxide powders were analysis by the analytical system used is a branded gas chromatography (GC) (IGC 1025 FL INTER SMAT)

3. RESULTS AND DISCUSSIONS

3.1Thermal Analysis of Precursor

The TG/DSC of the $La_{1-x}Sr_xAlO_{3-\delta}$ precursor powders were precipitated at pH =11 and at a heating rate of 10K/min in Fig1.The decomposition started below 100°C, which correspond to absorbed water, in a temperature range 100 - 600°C,this shows the decomposition of $La(OH)_3$, $Al(OH)_3$,$Sr(OH)_2$ to its amorphous oxide state[16] .The TG cuves which were observed in a the temperature rang 600-850°C are due to the removing of residual. The thermal decomposition behavior is an association of endothermic and exothermic effect. In the DSC cuves, the first decomposition step assignable removal of adsorbed and chemisorbed water is indicated by broad endothermic peak around 109°C.The second decomposition is shown by broad endothermic peak around 600°C which may be due to the final stage of decomposition $La(OH)_3$,$Al(OH)_3$,$Sr(OH)_2$[17].

Clear exothermic peak 717°C corresponds to the crystallization form.

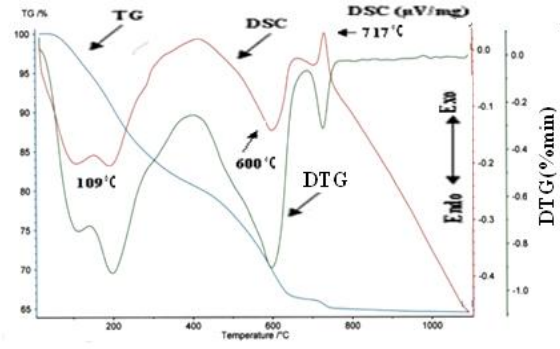

Figure 1.TGA-DSC curves of the hydroxide precursor x = 0.2

3.2Powder X-Ray Diffraction Studies

The XRD with Cu Kα radiation was used to characterize the phase purity and scanning rate set at 2°/min in 2Θ range between 10° and 70°. Fig.2 Show the patters of structure $La_{1-x}Sr_xAlO_{3-\delta}$ at x = 0, 0.1, 0.2 and 0.3 respectively calcined at 1000°C in static air for 6h. The phase analysis demonstrates of the $LaAlO_3$ showed complete crystallization peaks, which could be indexed on orthorhombic symmetry, and space R-3c confirmed the theoretical values of $LaAlO_3$ perovskite [18].Results demonstrated that values cell parameters of $La_{1-x}Sr_xAlO_{3-\delta}$ (0 <x<0.3) of the lattice parameters,' a' and 'c' and 'v (Tab.1) some what in the presence of Sr in the $LaAlO_3$ lattice. This increased in the 'a 'and' c' and' v' values may be ascribed to the replacement of the La^{3+}ion (1.023Å) by a relatively larger Sr^{2+}(1.18 Å) ion in the oxide matrix. As a comparison, the chemical stability of structure $La_{1-x}Sr_xAlO_{3-\delta}$(0<x<0.3) no apparent impurity phase this indicates good chemical compatibility.

Table 1. Cell parameters of $La_{1-x}Sr_xAlO_{3-\delta}$ (0 <x<0.3)

Oxides	a = b (Å)	C(Å)	V(Å3)
$LaAlO_3$	5.354	13.100	325.24
$La_{0.9}Sr_{0.1}AlO_{3-\delta}$	5.357	13.119	325.12
$La_{0.8}Sr_{0.2}AlO_{3-\delta}$	5.380	13.772	325.72
$La_{0.7}Sr_{0.3}AlO_{3-\delta}$	5.356	13.748	325.93

The XDR pattern of $La_{0.9}Sr_{0.1}AlO_{3-\delta}$ powders with different calcinating between 500°C-1000°C for 6H are shown in Fig. 3. After being heated at 500°C in air for 6H there are some weak XDR peaks with impurity peak disappear .Heating between 700-900 °C the XDR patterns are in good increased intensity of the X-ray peak and no other phases peak are

observed compared with results of Taspinar et al[19].The powders still amorphous. When increasing the heat to 1000°C,the diffraction peaks become stronger, reflecting greater crystallization.

It is noted that the strontium substitution leads to an increase in the a and b parameters.The c parameter for the composition x = 0, 0.1, increases significantly compared to the compositions x = 0.2, 0.3, probably due to the change from cubic to rhombohedral structure.

A small change in volume indicates the transition from cubic to rhombohedral form, the substitution by an ion (r_{Sr2+} = 1.44 Å), since the latter has a radius size closer to the radius size of lanthanum (r_{La3+} = 1.36 Å), which does not cause the volume change.

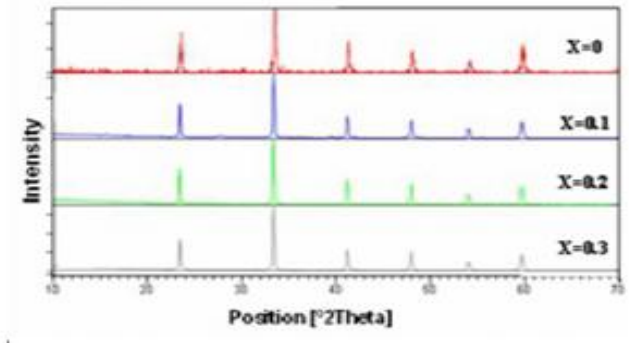

Figure 2. XDR patters of the $La_{1-x}Sr_xAlO_{3-\delta}$ (0<x<0.3) co-precipitation synthesized at 1000°C for 6h

3.3 Infrared Spectra

The important regions in the infrared spectra of the powders prepared by a co precipitation are (i) in a rang of (3600-3200 cm^{-1}) (assigned to the O-H),(ii) 1600 -950 cm^{-1}region (assigned to the N-O stretching vibrations),(iii) 950-400 cm^{-1} region (assigned mostly to the Al-OH and La-OH stretching vibrations) [20] .The IR spectra of precursor $La_{1-x}Sr_xAlO_{3-\delta}$(0<x < 0.3) shows in Fig .3.The spectrum between 3500 cm^{-1} is associated with the O-H stretch of intermolecular hydrogen bonds of molecular water [21] .The absorption band at 1600 cm^{-1} is attributed to moisture in the sample [22].The peaks due to the stretch vibration in NO_3^-at 1440 cm^{-1} (strong bands) are evident [23]. However, the peak at 616 cm^{-1} may be attributed to the characteristic M-O vibration.That is typical for the M-O (possible La-O and Al-O stretching frequencies) vibration for perovskite structure[24].

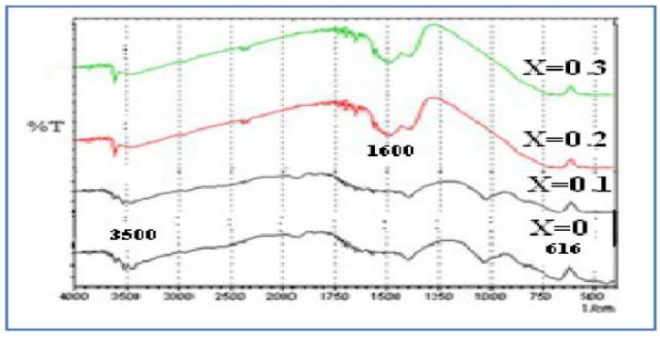

Figure 3.FTIR specter of series of as – formed samples of $La_{1-x}Sr_xAlO_{3-\delta}$(0<x<0.3)

3.4 Specifique Surface Area

Table 2 show the variation specifique surface area variation of the $La_{1-x}Sr_xAlO_{3-\delta}$(0<x<0.3) precursor powder was measured by B.E.T technique in nitrogen

Table 2. Variation of particle size with different specifique surface area

Oxides	Surface Area (m^2/g)	ØdBJH (nm)
$LaAlO_3$	7.6607	5.65
$La_{0.9}Sr_{0.1}AlO_{3-\delta}$	8.9650	6.67
$La_{0.8}Sr_{0.2}AlO_{3-\delta}$	11.6236	8.17
$La_{0.7}Sr_{0.3}AlO_{3-\delta}$	47.8660	33.82

The particle size was calculated from data of specifique surface area. In Fig. 5 specifique surface area of the $La_{1-x}Sr_xAlO_{3-\delta}$(0<x<0.3) adsorption isotherm have been increased by way of the Sr atomic ratio in $LaAlO_3$ either A site, isothermal adsorption dinitrogen allow highlighting the textural properties of materials. As part of this study, the shape of the isotherms Type IVis confirmed[25] in Fig. 4.

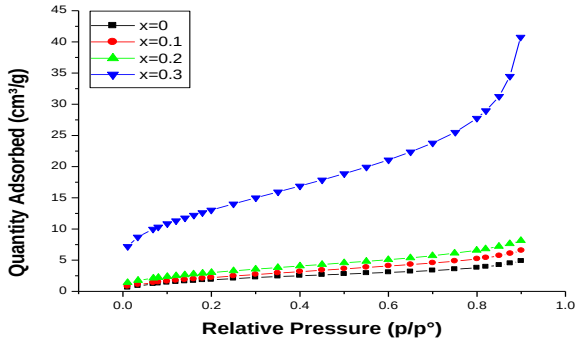

Figure 4.Typical N_2 adsorption isotherm of the $La_{1-x}Sr_xAlO_{3-\delta}$(x = 0, 0.1, 0.2, 0.3).

The BJH method provides access to the distribution of pore size Fig .5, justifying the presence of mesopores. The mesoporosity of the environment has a volume in the rangeof 0.1 to 0.4 $cm^3\ g^{-1}$ and the surface area is in the range of 10-100 $m^2\ g^{-1}$[26].

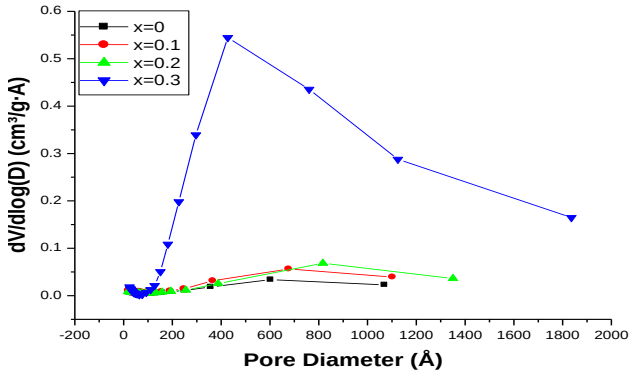

Figure 5. Pore volume distribution of the $La_{1-x}Sr_xAlO_{3-\delta}$(0<x<0.3) measuredB.E.T by method in N2 at 77.407K.

3.5 Catalytic Activity

3.5.1 Supply system

To carry out the catalytic tests, an experimental device has been implemented at the gas supply is carried out from three cylinders, the first of the methane CH_4 diluted in air and its concentration varies according to needs (0 to 2.5%) and the other two bottles contain one oxygen and the other pure nitrogen. The gas flows are adjusted using a flow meter system.

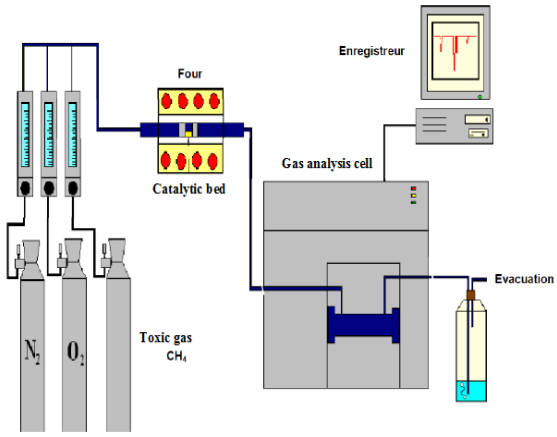

Figure 6.Gas chromatography system

3.5.2 Analytical system

All gases from methane (CO_2 , H_2O) conversion reactions were separated and quantified by gas chromatography analysis. The analytical system used is a branded gas chromatography (GC) (IGC 1025 FL INTER SMAT). We use helium as a carrier gas. At the exit of the column is a detector connected to a recorder when a component of the mixture passes through it, a peak appears on the recorder.

3.5.3 Reaction system

This system consists of a pyrex glass tube in U shape, the glass tube containing the catalyst is connected to the inlet to flow meters to inject the gas in proportion as the outlet to the CPG device. This system is housed inside a tubular furnace that allows the sample to be heated to a temperature of 500°C.

3.5.4 Analysis system

The output gas is collected directly to the gas chromatography unit. The CPG is applied to samples that are gaseous or likely to be vaporized without decomposing in the injector. The mobile phase is then a gas (helium, nitrogen, argon or hydrogen), called carrier gas, which continuously sweeps the column. The latter is placed in an oven. The separate chemical mixture is analyzed by flame ionization detector. At the exit of the column is a detector connected to a recorder when a component of the mixture passes through it, a peak appears on the recorder.

3.5.5 Calculation formulas

Methane is noted as a reference molecule, given its resistance to oxidation. The combustion of methane is governed by two different temperature-based mechanisms (T<500°C), the mechanism that describes the reaction is superficial. And the speed of reaction obeys the Rideal – Eleymodel [27].

$$r = KL\,.\,P\,CH4 \quad (1)$$

K_L: consistency of specific speed
P_{CH4}: partial methane pressure

At higher temperatures, methane reacts with the surface oxygenates supplied as the crystalline network reacts thus the overall speed of the reaction can be written in two parallel reactions

$$\boldsymbol{r} = KL\,.PCH4 + KCH4.PCH4 \quad (2)$$

K_{CH4}: consistency of methane adsorption equilibrium

3.5.6 Catalytic activity procedure

The oxidation reaction of methane on lanthanum - aluminate catalysts can be written as follows:

$$CH_{4\,(g)} + 2O_{2(g)} \xrightarrow[T=\,500°C]{La_{1-x}\,Sr_{\,X}\,AlO_3} CO_{2(g)} + 2H_2O_{(g)} \quad (3)$$

A catalyst quantity of 100 mg is placed between two caps of a U-shaped pyrex glass reactor [28]. To eliminate the possibility of high pressure losses in the reactor at the fill level, the catalyst powders obtained by synthesis have been well sieved and installed in the reactor support, then placed in a furnace at temperature T = 500°C. A residence time before each reaction, the catalyst is preprocessed for 15min at 500°C under 20% O_2 flight at a total flow rate of 100cc/sec.

The catalytic test starts first with a flow of He gas (15cc/5s) and then followed by a flow of oxygen (1cc/5s) mixed by a flow of CH_4 (1cc/6s) for a period of 5min at a temperature of 500°C until methane conversion. Finally, we accompany the kinetics of the CH_4 oxidation reaction for a catalyst temperature T = 500°C, based on chromatograms recorded by the brand-name gas chromatography (IGC 1025 FL INTER SMAT) device. The chromatograms recorded by the gas chromatography device (GC) show the conversion of methane into CO_2 and H_2O produced according to the different catalysts. The $La_{1-x}Sr_xAlO_{3-\delta}$ catalyst efficiency guide (x = 0.1, 0.2, and 0.3) for the methane oxidation reaction to CO_2 and H_2O is given by the following relationship:

$$hCO2 = \frac{hCO2}{hCO2} + hCH4 \quad (4)$$

h: peak height in chromatogram

Applying the relationship of the kinetic evolution of methane for conversion to CO_2 and H_2O[29], we processed the chromatogram peaks of the different catalysts $La_{1-x}Sr_xAlO_{3-\delta}$ (x = 0.1, 0.2, 0.3) using the intensity of each peak to measure methane conversion to CO_2 and H_2O.Fig.7 shows the

evolution of the conversion of methane to CO_2 over time in the presence of the different catalysts $La_{1-x}Sr_xAlO_{3-\delta}$ (x = 0.1, 0.2, 0.3)

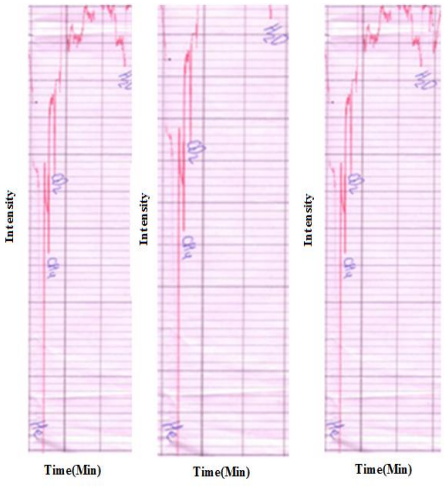

Figure 7.Evolution of the conversion of methane to CO_2over time in the presence of the different catalysts $La_{1-x}Sr_xAlO_{3-\delta}$ (x = 0.1, 0.2, 0.3)

Table 3. Conversion of methane to CO_2 and H_2O

Mixed oxide	Conversion to CO_2 (%)
$La_{0.9}Sr_{0.1}AlO_{3-\delta}$	28.94
$La_{0.8}Sr_{0.2}AlO_{3-\delta}$	29.26
$La_{0.7}Sr_{0.3}AlO_{3-\delta}$	36.36

We see from the peaks that represent the conversion of methane to CO_2 and H_2O after a given time, a rate of evolution in methane conversion each time the catalyst undergoes a change. We notice that the gaits present three parts[30]. The first part shows the stage of peak inactivation that is helium gas that plays the role of a carrier gas. The second part shows the activation of the catalyst which results in a rapid increase in the conversion rate of methane. This may be due to the increase in the number of CH_4 molecules adsorbed on the catalyst [31]. The third part pairs the CO_2 and H_2O peaks. The maximum catalytic activity of the different catalysts $La_{1-x}Sr_xAlO_{3-\delta}$ (x = 0.1, 0.2, 0.3), for the combustion reactions of CH_4, was observed on the surrogate samples (x = 0.1, 0.2, 0.3). A higher degree of substitution produces an increase in oxidation catalytic activity. The factor responsible for catalytic activity is related to the formation of a real oxide mixture due to the substitution of lanthanum by strontium inducing perovskite structure [32].

3.6 Scanning Electron Microscopy (M.E.B)

The snapshots of the Scanning electron microscopy of (a)$La_{0.9}Sr_{0.1}AlO_{3-\delta}$ (b)$La_{0.8}Sr_{0.2}AlO_{3-\delta}$ (c)$La_{0.7}Sr_{0.3}AlO_{3-\delta}$ after calcinations Fig.8 prepared by co-precipitation technique correspondingly of various forms and sizes are observe. In $La_{0.9}Sr_{0.1}AlO_{3-\delta}$, particles are in irregular morphologies and the powder is incompletely agglomerated[33]. However some particles agglomerate as shown in $La_{0.8}Sr_{0.2}AlO_{3-\delta}$.The structure of agglomerate is perhaps due low distribution of particles size Furthermore. In $La_{0.7}Sr_{0.3}AlO_{3-\delta}$ shows big hard spherical grains agglomerates of different sizes, Fig.5 which confirms this. The observed morphology was qualitatively the good lateness of their chemical composition.

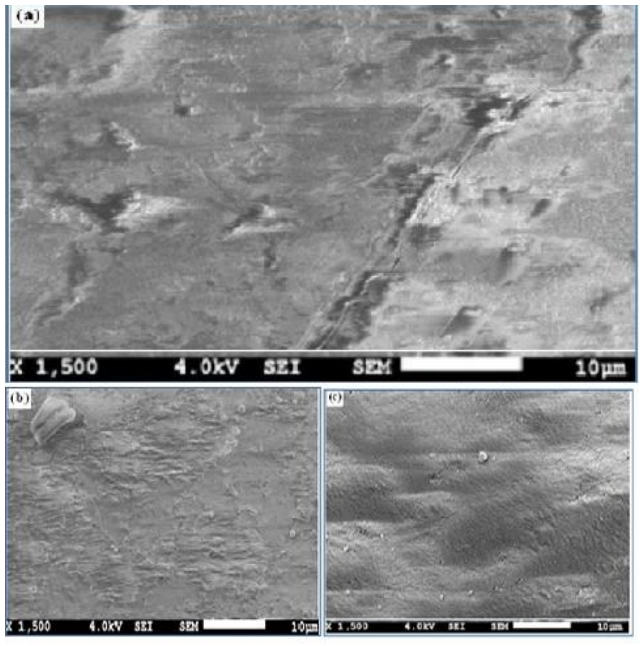

Figure 8..MEB micrographs of as – formed:
(a) $La_{0.9}Sr_{0.1}AlO_{3-\delta}$, (b) $La_{0.8}Sr_{0.2}AlO_{3-\delta}$ (c) $La_{0.7}Sr_{0.3}AlO_{3-\delta}$ (calcined at 1000°C 6h)

4.CONCLUSIONS

The powders of $La_{1-x}Sr_xAlO_{3-\delta}$(0<x<0.3) have been successfully prepared by the co - precipitation process.T
he catalytic activity has been well identified by applying the relationship of the kinetic evolution of methane for conversion to CO_2 and H_2O, we processed the chromatogram peaks of the different catalysts $La_{1-x}Sr_xAlO_{3-\delta}$ (x = 0.1, 0.2, 0.3) using the intensity of each peak to measure methane conversion to CO_2 and H_2O.The maximum catalytic activity of the different catalysts $La_{1-x}Sr_xAlO_{3-\delta}$ (x = 0.1, 0.2, 0.3), for the combustion reactions of CH_4, was observed on the surrogate samples (x = 0.1, 0.2, 0.3). A higher degree of substitution produces an increase in oxidation catalytic activity. The factor responsible for catalytic activity is related to the formation of a real oxide mixture due to the substitution of lanthanum by strontium inducing perovskite structure.

REFERENCES

[1] R.W. Simon, CE. Platt, A.E. Lee,., G.S. Lee, K. Daly, P., M. Swire, et al, Appl. Phys. Lett., **(1988),53**, 26, 2677-2679, https://doi.org/10.1063/1.100543.
[2] R. Spinical., P. Marini, Rossi, S.D., Faticanti, M., Porta, P.,J.Mol.Cata,A.Chem.,**(2001),176**,253-265. https://doi.org/10.1016/S1381-1169(02)00621-0.
[3] AN.Jain., SK .Tiwari., RN. Singh, . I.J. Of Hydrogen Energy **,(1997) 32.6** ,557-562. https://doi.org/10.1016/S0360-3199(96)00176-0
[4] A.Keshavaraja,AV.Ramaswamy,Thermochimica Acta.,**(1995), 254**,267-275. https://doi.org/10.1016/0040-6031(94)02057-U

[5] H.Ohboyashi,T .Kudo, Materials Research Bulletin .,**(1978)**,**13**-12,1409-1413.https://doi.org/10.1016/0025-5408(78)90133-2
[6]B. Lal , M.K. Raghunandan , M. Gupta , R.N. Singh,.I.J Of Hydrogen Energy.,**(2005),30**-7,723-729., https://doi.org/10.1016/j.ijhydene.2004.07.002
[7]Tarjomannejad.A., Farzi, A., Niaei, A., &Salari, D. Journal of Chemical Engineering. **(2016)**, **33, 2628**-2637. https://doi.org/10.1007/s11814-016-0108-4
[8]Damasceno.S., Trindade, F. J., Fonseca, F. C., de Florio, D. Z., & Ferlauto, A. S. Processing Technology., **(2022)**,**231**, 107255. https://doi.org/10.1016/jfuporoc.2022.107255.
[9]Vazhayil, A., Thomas, J., & Thomas, N**.** Journal of Electro of analytical Chemistry**.,(2022),918**,116426 https://doi.org/10.1016/j.jelechem.2022.116426
[10] Sim, Y., Kwon, D., An, S., Ha, J. M., Oh, T. S., & Jung, J.C.Molecular Catalysis**.,(2020),489**,110-925 https://doi.org/10.1016/cattod.2019.10.038
[11]Gihoon Lee , Ilho Kim , Inchan Yang , Jeong-Myeong Ha,Applied Surface Science **.(2018),429,**31,55-61 https://doi.org/10.1016/j.apsusc.2017.08.092
[12] A**.** Guemache, A. Bouchelaghem, M. Drif, F. Kahoul, L. Hamziou, Journal of New Materials for Electrochemical Systems**.,(2022),2**-25,15-148 https://doi.org/10.14447/jnmes.v25i2.a09
[13]Yujin Sim , Inchan Yang , Dahye Kwon , Jeong-Myeong Ha , Ji Chul Jung ,.Catalysis Today**.(2020),352**,1 134-139. . https://doi.org/10.1016/j.cattod.2019.10.038
[14] Ji, Q., Bi, L., Zhang, J., Cao, H., & Zhao, X. S. Energy & Environmental Science., **(2020)**, **13(5)**, 1408-1428. https://doi.org/ 10.1039/D0EE00092B
[15]G.N.Pirogova.,R.I.korosteleva.,N.M.Panich.,T.A.Lagutin a.,Y..Voronin,Russian Chemical bulletin.,**(1994),43**,4,551-554. https://doi.org/10.1007/BF0069982
[16]S.Bhattachearyya,SK.Praticher,Sinba,R.K,Bechere, R.C.,Ganguly, RI., Mater.lett**., (2002)**,**53,** 425-431, https://doi.org/10.1016/S0167-577X(01)00519-5
[17]A.Barabauskas,D.Jasaitis,A.Kareiva,Vib.Spectrosc**., (2002).28**, 263–275. https://doi.org/10.1016/S0924-2031(01)00157-6
[18] Yujie Ma, Peng Su, Yizhao Ge, Fangwai Wang,.Catalysis Letters. **(2022),152**, 2993–3003. https://doi.org/10.1007/s10562-021-03910-3
[19]Aliza Zahoor , Muhammad Isa , Tariq Mahmood ,.Physica B: Condensed Matter,(2023),652,1,414631. https://doi.org/10.1016/j.physb.2022.414631
[20]C.B.Sawyer,Js.Reed,J.Am.ceram.Soc.,**(2001),84,**6, 1241-1249. https://doi.org/10.1111/j.1151-2916.2001.tb00823.x
[21] Baek, J., Jin, Q., Johnson, N.S. electrolysis towards hydrogen peroxide. Nat Commun **(2022),13,**7256 https://doi.org/10.1038/s41467-022-34884-4
[22] S. Lin, -B.Wen, J. Am. Ceram. Soc., **(2002), 85**, 1467–1472, https://doi.org/10.1111/j.1151-2916.2002.tb00298.x
[23]Turgut M. Gür Prog. Solid State Chem., **(2016).54**,164 https://doi.org/10.1016/j.pecs.2015.10.004
[24]Gupta,M.,Rambadey,O.V., Shirbhate, S. C., Acharya.The Journal of Physical Chemistry C.,**(2022)**, **126(48),** 20251-20262. https://doi.org/10.1021/acs.jpcc.2c06473
[25]Calzaferri, G., Gallagher, S. H. Microporous and Mesoporous Materials., **(2022)**, *330*, 111563. https://doi.org/10.1016/j.micromeso.2021.111563
[26] Alsaiari, M., Younus, A. R., Rahim, A., Alsaiari, R., & Muhammad, N. MicrochemicalJournal., **(2021),**165, 106171. https://doi.org/10.1016/j.microc.2021.106171
[27] Zhang, X., Dai, L., Liu, Y., Deng, J., Jing, L., Wang, Z. Applied Catalysis B:Environmental., **(2021)** *285*,119804. https://doi.org/10.1016/j.apcatb.2020.119804
[28] Khalilzadeh, M. A., Tajik, S., Beitollahi, H., & Venditti, R.A.Industrial&EngineeringChemistryResearch., **(2020)**,**59(10)**, 4219-4228.https://doi.org/10.1021/acs.iecr.9b06214
[29]Navarro, M. V., Plou, J., López, J. M., Grasa, G.International Journal of Hydrogen Energy., **(2019)**, 44(25), 12617-12627.https://doi.org/10.1016/j.ijhydene.2018.12.056
[30]Li, X., Sun, Y., Xu, J., Shao, Y., Wu, J., Xu, X. Nature Energy., **(2019)**,***4*(8**), 690-699. https://doi.org/10.1038/s41560-019-0431-1
[31] Zhao, C., Xi, M., Huo, J., He, C., & Fu, L. Chinese Chemical Letters., **(2023)** ,***34*(1)**, 107213. https://doi.org/10.1016/j.cclet.2022.02.018
[32] Zhang, M., Zou, P., Jeerh, G., Sun, B., Walker, M., & Tao, S. Advanced Functional Materials., **(2022)**,**32(38)**, 2204881.https://doi.org/10.1002/adfm.202204881
[33] Wang, Y., Zhong, Y., Luo,. npj Quantum Materials., **(2019)**. **4(1),** 15. https://doi.org/10.1038/s41535-019-0156-1